Graded Vertical Phase Separation of Donor/Acceptor Species for Polymer Solar Cells

Anna Loiudice, [a,b] *Aurora Rizzo,* [b, c*] *Gianluca Latini,* [b] *Concetta Nobile,* [c] *Milena de Giorgi,* [c] *and Giuseppe Gigli* [a,b,c]

[a] Dipartimento di Ingegneria dell'Innovazione, Università del Salento, Via Arnesano, I-73100 Lecce, Italy

[b] Center for Biomolecular Nanotechnologies @UNILE Istituto Italiano di Tecnologia, Via Barsanti, 73010 Arnesano (LE), Italy

[c] NNL CNR- Istituto Nanoscienze, c/o Distretto Tecnologico, via per Arnesano 16, I-73100 Lecce, Italy

*Corresponding author: Tel: 0039-0832-298211. Fax: 0039-0832-298237

E-mail: aurora.rizzo@nano.cnr.it.

Abstract

The donor/acceptor inter-mixing in bulk heterojunction (BHJ) solar cells is a critical parameter, often leading to irreproducible performance of the finished device. An alternative solution-processed device fabrication strategy towards a better control of the micro/nano-structured morphology consists in a sequential coating of the donor (e.g., poly-(3-hexylthiophene), P3HT) and acceptor (e.g., [6,6]-phenyl-C_{61}-butyric acid methyl ester, PCBM) from orthogonal solvents. We demonstrate that, in spite of the solvent orthogonality, this technique does not lead to a well-defined bilayer with a sharp interface, but it rather results in a graded vertical phase-separated

junction, resulting from the diffusion of the PCBM in the P3HT bottom layer. We are able to control the diffusion of PCBM, which occurs preferentially in the amorphous P3HT domains, by easily varying the ratio between crystalline/amorphous domains in the P3HT. Such a ratio can be simply modified by changing the solvent for P3HT. We show that the donor-acceptor diffused bilayer (DB) junction is an intermediate structure which combines both advantages of the well-defined bilayer and conventional BHJ configurations. Indeed, the DB device geometry ensures the good reproducibility and charge percolation, like the well-defined bilayer, while preserving the interpenetration of the donor and acceptor species, resulting in an efficient charge separation, characteristic of the BHJ. Overall the annealed DB device geometry can be assimilated to a graded BHJ with an improved reproducibility and mean power conversion efficiency (PCE) of 3.45%, higher than that of the standard BHJ devices of 3.07%. Furthermore, we demonstrate the highest performance for the as-cast DB device with a PCE of 2.58%. It is worthy of note that our DB device exhibits improved open circuit voltage, fill factor, series and shunt resistances, which denote that the vertically phase separated DB junction ensures improved charge percolation.

Keywords: Photovoltaic devices, bilayer, graded diffusion, solution processed, micro/nano-morphology, bulk heterojunction.

1. Introduction

Current state-of-the-art of solution-processed organic photovoltaic (OPV) cells is based on the so-called BHJ architecture, consisting of an active layer that is a mixture of electron-donor and -acceptor species forming an interpenetrating network structure where photocharges are generated efficiently.[1-3] The BHJ OPV devices are regarded as the most efficient configuration for the

plastic PV industry.[4] Polymer solar cells have been moving rapidly toward large scale manufacture.[5] Many recent progresses have been made by using novel methodologies based on roll to roll[6] or fast speed deposition methods[7], but there are still major obstacles towards the commercialization of such devices, that limit the device performance such as the poor control over the fabrication process.[8] As a consequence there is a need to identify new routes to optimize and control the morphology for high-performance devices, which could possibly reach the minimum requirements for applications.[9,10]

The as-cast blend morphology is generally believed to be a molecular mixture of P3HT and PCBM,[11] in which the PCBM domains are kinetically trapped in the P3HT-rich domains. The inefficient charge transport pathways in these films, due to incomplete phase segregation, hinder the charge extraction towards their respective electrodes and results in low efficiencies. In order to improve the charge percolation through a reorganization of P3HT and PCBM phases, the BHJ system is often subject to processes that modify the micro/nano-structure such as thermal[12,13] or solvent annealing,[14,15] addition of a third component (i.e. dithiols),[16,17] or solubilisation in a mixture of solvents.[18,19] However, despite all these studies and progresses, different research groups using the same processing recipe for producing polymer/fullerene thin-film photovoltaic devices reports very different results, indicating that there are still processing parameters that have not yet either correctly identified or properly learned to control.[8]

Recently, Ayzner et al.[20] have reported that solution-processed thermally annealed P3HT/PCBM bilayer solar cells can be almost as efficient as BHJ cells. In that work an orthogonal solvent combination (o-dichlorobenzene, o-DCB, and dichloromethane, DCM) was used to process a PCBM layer on top of a P3HT layer. The authors presented indirect evidence that this fabrication method led to the formation of a well-defined bilayer with a sharp interface,

however several recent investigations have demonstrated that the interdiffusion of PCBM into P3HT produces a partial intermixed heterojunction directly during the deposition.[21-27] They have found that upon thermal annealing, PCBM becomes preferentially miscible and mobile in disordered and amorphous P3HT regions, driving the interdiffusion of P3HT and PCBM to completion without disrupting the ordered domains with lamellar stacking of P3HT chains.

In this study, we demonstrate that the inter-diffusion of PCBM into the P3HT under-layer can be controlled by a facile tuning of the ratio between crystalline and amorphous phases in the P3HT. Such a ratio can be easily varied by switching from a relatively high-boiling point solvent, i.e., o-DCB, to a lower one, i.e., chlorobenzene (CB).[28,29] This allows reaching a graded vertical phase separation between the P3HT and PCBM, which leads to a better reproducibility of the fabrication process and to a PCE comparable with the standard BHJ device configuration: the mean value of the PCE is 3.45% with a standard deviation of ±0.10% for the annealed DB devices, whereas the mean PCE is 3.07% for the BHJ devices with a standard deviation of ±0.30%. The as-cast (non-annealed) device shows a PCE of 2.58%, demonstrating that the complete diffusion of PCBM occurs immediately upon the deposition.

To correlate the device performances with the micro/nano-structure of P3HT and to further deepen our understanding on the DB device, we report a systematic characterisation, which comprises cross-section scanning electronic microscopy (SEM) images and transient photoluminescence measurements.

2. Experimental Details

For the fabrication of the DB solar cells, a Poly(3,4-ethylenedioxythiophene)-poly(styrenesulfonate) (PEDOT:PSS) layer was deposited onto an ITO/glass substrate. Then, the

P3HT (Rieke metals, > 98% regioregular) solution in CB was spin-casted onto the PEDOT:PSS layer and was allowed to dry in glove box for 20 min. Then, the PCBM layer was spin-casted from dichloromethane. The annealed DB devices were prepared by annealing the complete stack at 150°C for 10min in a glove box, wherein a digital controllable hotplate was used under an inert gas condition. For the BHJ solar cells, a solution of P3HT:PCBM (1:0.8 wt % in CB) blend was spin-coated at 700 rpm for 45s and dried under a Petri dish. The obtained film was annealed at 110°C for 10min.

To complete the device structure a LiF/Al electrode was thermally evaporated at low pressure ($<1\times10^{-6}$ Torr). The active area of the devices was 0.03cm^2. Current density versus voltage characteristics (J-V) were measured using a Keithley 2400 sourcemeter both in dark and under AM 1.5-G illumination with an incident power of 100 mW/cm^2. All devices were tested under ambient conditions. A set of ten devices was tested for each structure.

Absorption measurements were performed using a Varian Cary 5000UV-visible spectrometer in ambient conditions. High-resolution scanning electron microscopy (HR-SEM) characterization was performed with a FEI NOVAnanoSEM200 microscope. Typically, the images were acquired at an accelerating voltage of 5 kV. The samples were prepared by spin coating the polymers on Si substrates. For cross-section measurements the samples were immersed in liquid nitrogen and then fractured.

Time-resolved photoluminescence (TRPL) experiment were performed at room temperature by exciting the samples with the second harmonic (400 nm) of a Ti:sapphire pulsed laser (80 fs pulses at 80 MHz repetition rate). Average power on the sample was 4mW with a 200-400μm wide spot. The signal was collected by a spectrograph 0.5 m focal length and detected by a streak camera (temporal resolution of about 12 ps). For this experiment a series of samples with varying

P3HT thickness were fabricated on glass substrate following the same procedure (materials, solvents, annealing conditions etc.) as for the devices except for the fact that the architecture of the samples only consisted of a sequential deposition of a layer of P3HT (thickness 80, 170, 400 and 700nm) and PCBM (40nm) on glass. Film thicknesses were measured by using an Alfa-Step IQ profilometer. Samples were then encapsulated in inert conditions. This allowed performing the measurements in air at room temperature preventing photo-oxidation which was carefully monitored observing no degradation measurement after measurement.

3. Results and Discussion

Fig. 1 shows the current density–voltage curves (under illumination and in the dark) of the as-cast DB, annealed DB and standard BHJ solar cells with the best performance. The photovoltaic performances are summarized in Table 1 together with the values averaged over the set of devices tested. The annealed DB device exhibits a maximum PCE of 3.60% under AM1.5 conditions (open-circuit voltage V_{OC}=0.60 V, short-circuit current density J_{SC}=8.49 mA×cm^{-2}, fill factor FF=72%), which is comparable with the PCE obtained for the best BHJ device (3.76%). Additionally, good reproducibility of device performance is accomplished by this structure (Table 1): standard deviation of ±0.10% for the annealed DB devices with mean value of the PCE=3.45%, whereas, for the BHJ devices, standard deviation of ±0.30% with mean PCE=3.07%.

In order to have a better control on the micro/nano-morphology of P3HT, as will be explained later, in the fabrication of our device we use a lower boiling point CB (132°C), instead of higher boiling point o-DCB (180°C), as a solvent for the P3HT. In Table 1 we compare the photovoltaic parameters of two reference devices where the P3HT is spun from o-DCB with or

without the annealing treatment. It can be readily noted that the as-cast DB from o-DCB has a much lower PCE than the annealed one and a PCE ca. 50% lower than the device as-cast from CB. It is worthy of note that our as-cast DB device has the highest efficiency achieved in solution processed as-cast solar cells to date, which is important in the frame of low temperature processing conditions for plastic electronic production.

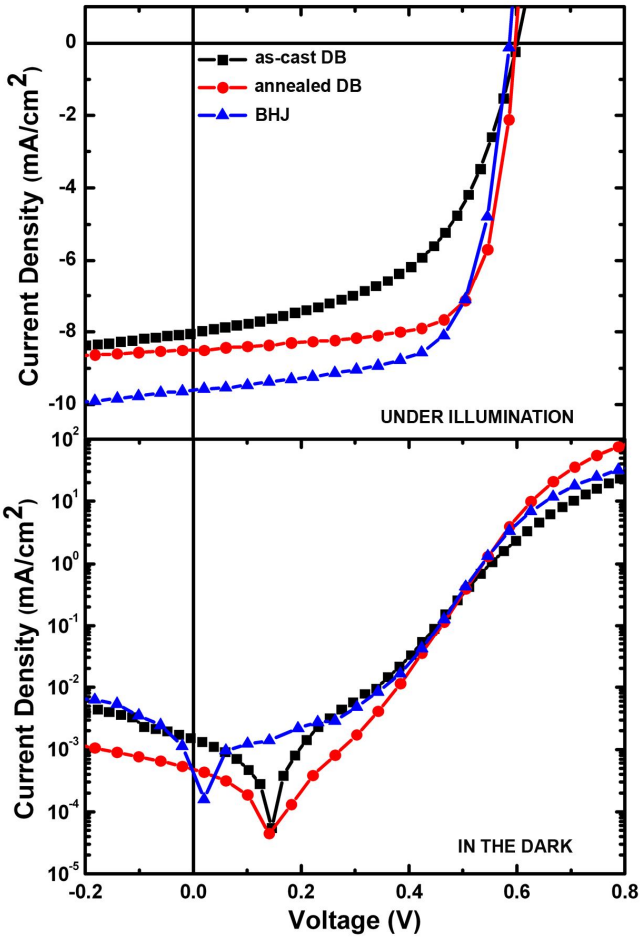

Figure 1. Current Density–Voltage characteristics under illumination (top panel) and in the dark (bottom panel) for the best devices made with as-cast DB (black line - squares), annealed DB (red line - circles) and BHJ structure (blue line – triangles).

Table 1. Performance parameters of the different structures under 100mW/cm^2 A.M. conditions.

reference		J_{SC}(mA/cm^2)	FF	V_{OC}(V)	PCE(%)	R_{sh}(Ωcm^2)	R_s(Ωcm^2)
This work	**BEST as-cast DB**	8.19	0.53	0.60	2.58	1.00×10^5	25.06
	Agv.	8.00±0.20	0.54±0.01	0.58±0.01	2.51±0.10		
	BEST annealed DB	8.49	0.72	0.60	3.60	3.60×10^5	9.22
	Agv.	8.11±0.20	0.71±0.01	0.60±0.01	3.45±0.10		
	BEST BHJ	9.56	0.67	0.58	3.76	3.50×10^4	14.23
	Agv.	7.84±0.70	0.66±0.02	0.59±0.01	3.07±0.30		
***Lee et al.*[26]**	**as-cast DB from o-DCB**	6.54	0.50	0.40	1.31	-	-
	annealed DB from o-DCB	8.61	0.74	0.62	3.80	-	-

We calculate the series resistance (R_s) and shunt resistance (R_{sh}) from the inverse slope of J-V dark (Fig.1) characteristics at V=0V and V=V_{OC} respectively.

The results indicate that the R_s of the as-cast DB is largely diminished by the thermal annealing; this improvement is a direct consequence of changes in the active layer micro/nano-morphology. Indeed, upon thermal treatments, the crystallization of the conjugated polymer backbones leads to an enhanced hole mobility and, simultaneously, the re-crystallized polymer forces the PCBM to migrate towards each other forming interconnected percolating networks in active layers.[30-33] Accordingly the two phases become more pure, forming an interpenetrating pathway for charges, in the pure PCBM and P3HT phases, which results in better transport properties, i.e. series and shunt resistances.

From the current density vs voltage characteristics in the dark, we extrapolate the saturation current density (J_0) by fitting ($V-JAR_s$) versus $\ln(J-(V-JAR_s)/AR_{sh})$ from the y-axis intercept (where J is the current density, V is the applied voltage and A is the area of the solar cell).[34]

The annealed DB shows a $J_0=8.5\times10^{-9}$ A/cm^2, while the BHJ of 4.7×10^{-8} A/cm^2. We consider the decreased J_0 to be indirect evidence for the fact that a thin layer of P3HT and PCBM indeed

serve as charge-blocking layer in the DB architecture. This is also corroborated by an increase in the FF (Table 1), which implies a higher maximum power point current as a result of delayed turn-on of current injection due to the charge-blocking effect.

The V_{OC} of the DB is higher than that of the standard BHJ, as summarized in Table 1. Similar enhancement of V_{OC} via solvent treatment has been reported and explained by the presence of vertical phase segregation in active layer.[35] It is known that normally the V_{OC} of the device with a bilayer structure is higher than that of BHJ OPV because both electrons and holes can more easily be transported to an appropriate electrode without recombination.[36] Additionally, the annealed DB architecture increases the R_{sh} by an order of magnitude, if compared with the standard BHJ, while lowering the R_s of ca. 35%. The shunting resistance is an important factor to evaluate the leakage current level in a solar cell. In the model of an ideal solar cell, the shunting resistance is infinity. In the real devices, the recombination losses reduce the shunting resistance to a finite value. Our results show that the higher V_{OC} is assigned to larger R_{sh}, indicating that the DB architecture (both as-cast and annealed one) is a device based on vertical phase segregation.

In order to assess the effect of the polymer nanostructure on the device performances, we compare the UV-Vis absorption spectra of the P3HT spin-coated from CB and o-DCB (Fig. 2). The solid-state photophysics of organic systems is heavily affected by their nanostructure.[37] In the case of P3HT the absorption spectrum is a useful and ease-to-measure tool to analyze the nanostructure of polymeric thin films. A quantitative estimation of the P3HT fraction made up of aggregates, but also of the degree of excitonic coupling within the aggregates can be determined by mean of a weakly interacting H-aggregate model.[38,39] The film absorption spectrum is the superposition of two components: a low-energy feature characterized by a modified Condon

vibronic series associated to the more ordered molecules which form weakly interacting H-aggregate states (crystalline regions) and a high-energy feature that resembles the spectrum of P3HT in diluted solutions and, then, assigned to more disordered chains which form intrachain states only (amorphous regions).[40] Using the model introduced by Spano,[29] is thus possible to extract the exciton bandwidth of the aggregates, *W*, and the fraction of the spectrum made up of aggregate, *%A*.

Fig. 2 shows the absorption spectra of the P3HT spin-coated from CB and o-DCB solvent with the relative fitting of the H-aggregate feature and the extrapolated component from the disordered molecules.

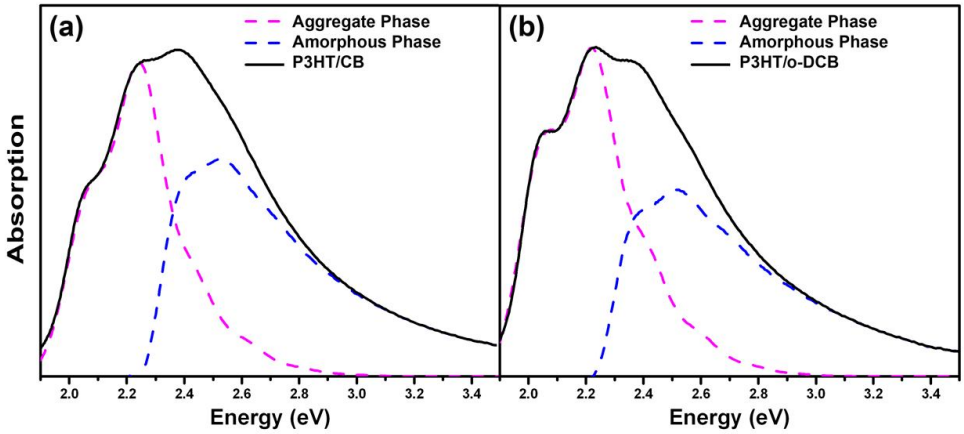

Figure 2. Absorption spectra of P3HT spun from CB (a) and o-DCB (b).

The results demonstrate that the film spun from CB, because of the lower boiling point, exhibits larger *W* (148 meV) and hence shorter effective conjugation lengths, i.e, a lower crystalline quality; on the contrary the film deposited from o-DCB shows lower *W* (92 meV) with correspondingly longer effective conjugation lengths, i.e. a higher crystalline quality.

Furthermore, the film spun from CB has a lower proportion of crystalline aggregated regions of 51% compared with that spun from o-DCB of 56%, as expected. We demonstrate that the diffusion of the PCBM in the P3HT under-layer is strongly influenced by the fraction of aggregate/amorphous regions; namely even though the PCBM solvent, DCM, is a poor solvent for P3HT it may cause swelling of the P3HT and allow the PCBM inter-diffusion, which occurs without decreasing the order of the P3HT aggregate domains, consequently a higher percentage of amorphous domains would results in a better diffusion of the PCBM.

The interdiffusion grade of the PCBM in the P3HT underlayer at different conditions is investigated using cross-sectional SEM and transient PL measurements. Fig. 3 shows the SEM images of P3HT/PCBM in DB or BHJ configuration deposited from CB onto silicon substrates. The comparison between the as-cast DB (Fig. 3a), the annealed DB (Fig. 3b) and the standard BHJ (Fig. 3c) images demonstrates that the intermixing of the P3HT and PCBM occurs in all the cases. The images of the as-cast DB and the annealed DB do not reveal the presence of a well-defined interface between the P3HT and PCBM. Thus we can conclude that both as cast and annealing preparation conditions lead to an intermixed phase film, which results from the diffusion of PCBM, rather than a well-defined bilayer.

Most notably, the as-cast and annealed DBs are not uniform and a phase separation of the P3HT and PCBM into bicontinuous morphology is evident. Some differences can be gathered between the annealed and the as-cased DB. In particular smaller features, at the microscale, on the annealed DB can be noted, which can offer a more extended active area for the charge separation at the interface between P3HT and PCBM.

These results clearly show that the bilayer nature of the sample is vanished, due to the complete interdiffusion of the P3HT and PCBM and that a uniform layer is formed.

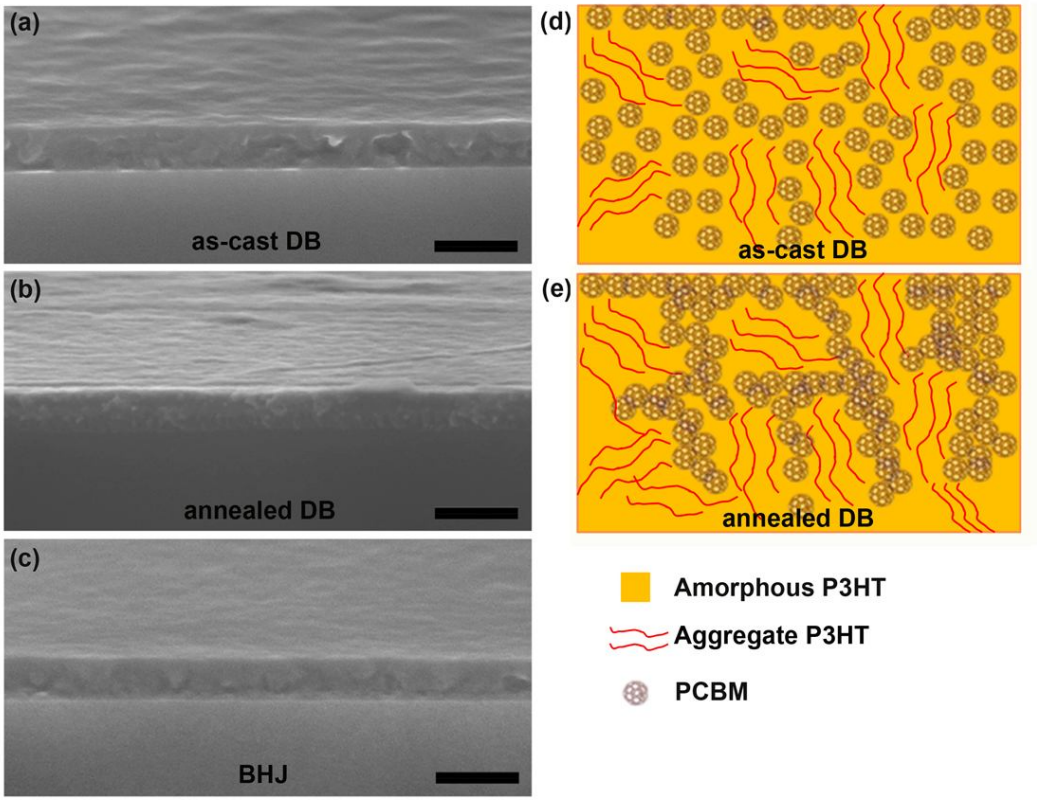

Figure 3. Cross-section SEM images of a) the as-cast DB, b) annealed DB and c) BHJ; Scale bar 100nm. Schematic representation of d) the as-cast DB and e) annealed DB.

Accordingly to previously-reported X-ray scattering data,[27] we can conclude that PCBM immediately upon the spin-coating penetrates though the entire P3HT layer; during the annealing step the PCBM can be driven out from the domain of P3HT, resulting in the formation of interpenetrating pathway for the electrons in the pure PCBM phase and for the holes in the pure P3HT phase. All these factors contribute to the improvement in the performances of the annealed DB. For clarity a sketch of the process is reported in Fig. 3d and 3e, and respectively represents the active layer morphology of the as-cast and annealed DB.

In order to better quantify the extension of the diffusion of the PCBM into the P3HT layer we carry out PL quenching measurements on samples with different P3HT layer thickness (details on the sample fabrication in the Experimental Details section).

In general, the PL of P3HT is dominated by a single emissive specie, i.e., weakly coupled H-aggregates[40] in the spectral window between 1.4 and 2.0eV. The optical emission is characterized by a monoexponential decay with τ~500ps at RT.[38] Because of the efficient charge transfer to the PCBM the addition of this one to P3HT induces PL quenching and a faster decay.[2]

We perform time-resolved PL measurements on such DB architecture exciting at relatively grazing incident angles (50-55º) from the P3HT side (Forwards, F) and from the PCBM side (Backwards, B). Considering the absorption coefficient to be ca. 1×10^5 cm^{-1} at the excitation energy used here (i.e., 3.1 eV), it can be estimated that ~50% of light is absorbed in the first ~40 nm of the film. So, when exciting from the P3HT side the measurement is selectively sensitive to the glass/P3HT (encapsulated samples) interface, while when exciting B, being PCBM very little absorbing at 3.1 eV, the measurement is sensitive to the PCBM/P3HT interface. In case of a relatively sharp interface the F measurement should provide results close to the P3HT-only sample, while the B measurement should provide quenched PL.

In Fig. 4a we report representative time-resolved PL measurements corresponding to the spectral window comprised between 1.4 and 2.0eV for the series of as-cast DB samples plus annealed P3HT and P3HT:PCBM BHJ. As expected P3HT displays a monoexponential decay with τ =440ps in agreement with previous reports. When PCBM is added, efficient quenching is observed and the decay is significantly faster.

No significant differences between the F and B measurements are observed. This indicates that the intermix between P3HT and PCBM has to be very pronounced and the experiment is not sensitive enough to detect such smooth interface. Surprisingly, no significant differences are observed even for the very thick P3HT layers (700 nm) confirming a deep PCBM interdiffusion. When PCBM is deposited on thicker P3HT bottom layer the quenching is less efficient and the PL decay is slower.

In Fig. 4b we resume the results of the whole series of measured samples as a function of the P3HT thickness. We report the value τ evaluated as the time for which the PL intensity drops by e^{-1} after excitation. For comparison we also report $\tau = (34\pm4)$ ps as estimated for the annealed P3HT:PCBM BHJ. Observations reported above for the as-cast sample series apply to the annealed samples too, i.e., no differences between F and B measurements, monotone increasing trend of τ with P3HT thickness, but we also observe that the decay is systematically slower for the annealed samples. This is interpreted as the result of phase segregation between the two components P3HT and PCBM induced by the annealing. Still, the interface remains smooth and PCBM deeply penetrated the P3HT since the F and B experiments provide identical results.

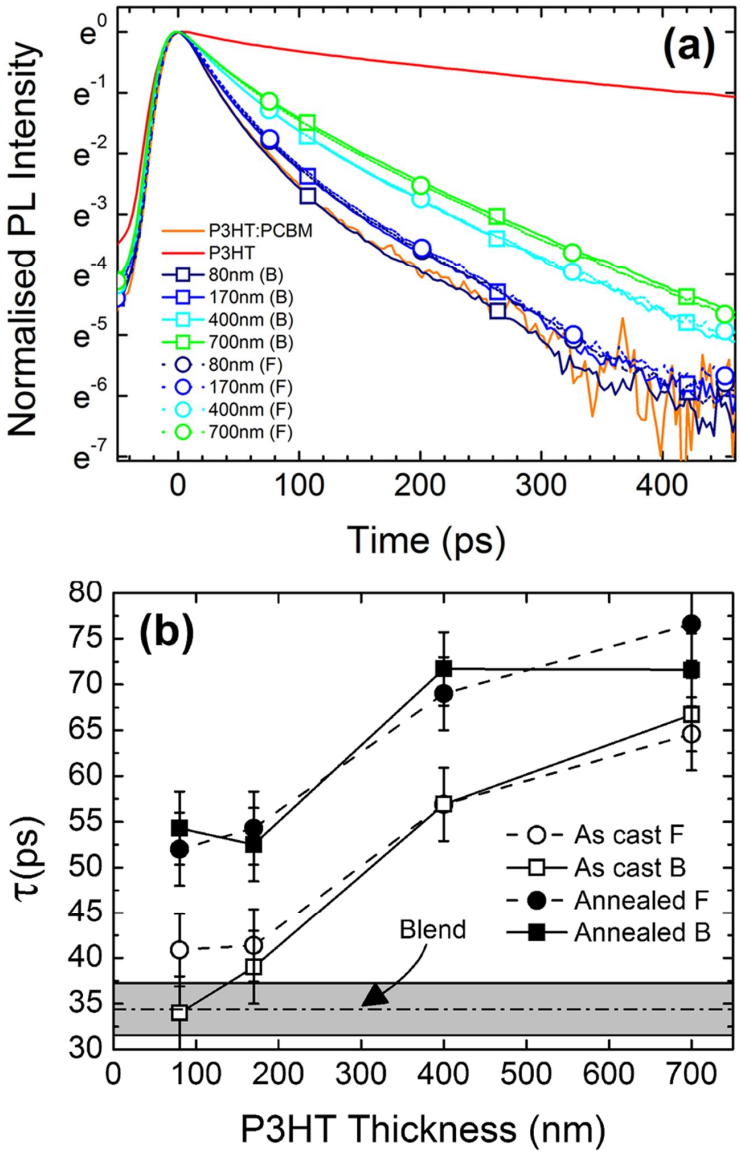

Figure 4. (a) PL time decay of as-cast films with different thickness compared with P3HT only and the annealed P3HT:PCBM BHJ. Decays are reported for samples excited from the PCBM side labelled as B (squares) and from the P3HT side labelled as F (circles). (b) PL time decay of

the all series of samples measured evaluated as the time for which the PL intensity drops by e^{-1} after excitation. Error bar (4ps) is the standard deviation for three independent measurements.

This analysis, in conjunction with the electrical characterization, demonstrates that the PCBM rapidly percolates throughout the P3HT film (spin-cast from CB) without need of thermal annealing. The improvement in the annealed DB device performance is due to completion of phase segregation driven by thermal annealing, resulting in improved charge percolation/extraction, FF and V_{OC}. Thus, much akin to the BHJ, the annealing is responsible for the improvement in the efficiency. However, the mechanism for the formation of the interpenetrating network is subtly different to that of the BHJ. Instead of phase separation at the time of the spin-coating and annealing, in these solutions processed devices, the network arises from the complete diffusion of PCBM into a layer of organized P3HT, that probably is the reason of the better reproducibility of the performance of this type of architecture.

1. Conclusions

In conclusion, we show that sequential solution processing of P3HT and PCBM layers produces an intermixed heterojunction even without thermal annealing. Therefore, the PCBM diffuses into a framework established by the ordered domains of P3HT. The lower is the crystalline quality of the P3HT, the more rapid is the complete diffusion of the PCBM. As a result, the thermal annealing has a negligible effect on the device performances, which results in the higher PCE for the as-cast DB.

The improved photovoltaic parameters, V_{OC} and FF, device resistances, R_s and R_{sh}, and reproducibility, support our finding that diffused bilayer (DB) junction is an intermediate

structure which combines both advantages of the well-defined bilayer and conventional BHJ configurations. Our results demonstrate that the sequential solution processing of the active layers in organic solar cells may be a viable and potentially more robust route to the creation of next generation devices when compared to the current BHJ techniques.

Acknowledgements

This work was supported by the Italian projects Rete Nazionale di Ricerca sulle Nanoscienze ItalNanoNet (FIRB reference number RBPR05JH2P), EFOR-Energia da FOnti Rinnovabili (Iniziativa CNR per il Mezzogiorno L. 191/2009 art. 2 comma 44), and the European project ESCORT- Efficient Solar Cells based on Organic and hybrid Technology (7th FWP- reference number 261920).

References

[1] J.J.M. Halls, C. A. Walsh, N.C. Greenham, E.A. Marseglia, R.H. Friend, S.C. Moratti, A.B. Holmes, Nature 376 (1995) 498.

[2] N.S. Sariciftci, L. Smilowitz, A. J. Heeger and F. Wudl, Science 258 (1992) 1474-1476.

[3] X. Yang, J. Loos, S.C. Veenstra, W.J.H. Verhees, M.M. Wienk, J.M. Kroon, M.A.J. Michels and R.A.J. Janssen, Nano Lett. 5 (2005) 579.

[4] F.C. Krebs, T. Tromholt and M. Jørgensen, Nanoscale 2 (2010) 873-886.

[5] F.C. Krebs, J. Fyenbo, D.M. Tanenbaum, S.A. Gevorgyan, R. Andriessen, B. van Remoortere, Y. Galagand and M. Jørgensen, Energy & Environmental Science 4 (2011) 4116-4123.

[6] M.V. Madsen, K.O. Sylvester-Hvid, B. Dastmalchi, K. Hingerl, K. Norrman, T. Tromholt, M. Manceau, D. Angmo and F.C. Krebs, J. Phys. Chem. C 115 (2011) 10817-10822.

[7] J. Alstrup, M. Jørgensen, A.J. Medford and F.C. Krebs, ACS Appl. Mater. Interfaces 2 (2010) 2819-2827.

[8] M.K. Riede, K.O. Sylvester-Hvid, M. Glatthaar, N. Keegan, T. Ziegler, B. Zimmermann, M. Niggemann, A. Liehr, G. Willeke, A. Gombert, Prog. Photovolt: Res. Appl. 16 (2008) 561-576.

[9] Y. Yao, J. Hou, Z. Xu, G. Li, Y. Yang, Adv. Funct. Mater. 18 (2008) 1783.

[10] S.S. van Bavel, M. Bärenklau, G. de With, H. Hoppe, J. Loos, Adv. Funct. Mater. 20 (2010) 1458.

[11] D. Chirvase, J. Parisi, J. C. Hummelen, V. Dyakonov, Nanotechnology 15 (2004) 1317-1323.

[12] W.L. Ma, C.Y. Yang, X. Gong, K. Lee, A.J. Heeger, Adv. Funct. Mater. 15 (2005) 1617-1622.

[13] H. Hoppe, N.S. Sariciftci, J. Mater. Chem. 16 (2006) 45-61.

[14] Y. Kim, S. Cool, S.M. Tuladhar, S.A. Choulis, J. Nelson, J.R. Durrant, D.D.C. Bradley, A.R.K. Giles, I. McCulloch, Nature Materials 5 (2006) 187-203.

[15] J. Jo, S.I. Na, S.S. Kim, T.W. Lee, Y. Chung, S.J. Kang, D. Vak, D.Y. Kim, Adv. Funct. Mater. 19 (2009) 2398-2406.

[16] J.K. Lee, W.L. Ma, C.J. Brabec, J. Yuen, J.S. Moon, J.Y. Kim, K. Lee, G.C. Bazan, and A.J. Heeger, J. Am. Chem. Soc. 130 (2008) 3619-3623.

[17] Y. Liang, Z. Xu, J. Xia, S.T. Tsai, Y. Wu, G. Li, C. Ray, and L. Yu, Adv. Mater. 22 (2010) 1-4.

[18] S.H. Park, A. Roy, S. Beaupre, S. Cho, N. Coates, J.S. Moon, D. Moses, M. Leclerc, K. Lee, and A. J. Heeger, Nature Photonics 3 (2009) 297-303.

[19] C.W. Chu, H.C. Yang, W.J. Hou, J.S. Huang, G.Li, Y. Yang, Appl. Phys. Lett. 92 (2008) 103306.

[20] A.L. Ayzner, C. J. Tassone, T.S. Holbert, B.J. Schwartz, J. Phys. Chem. C 113 (2009) 20050-20060.

[21] D.H. Wang, D-G. Choi, K.-J. Lee, S.H. Im, O.O. Park, J.H. Park, Org. Electron. 11 (2010) 1376-1380.

[22] B.A. Collins, E. Gann, L. Guignard, X. He, C.R. McNeill, H. Ade, J. Phys. Chem. Lett. 1 (2010) 3160-3166.

[23] N.D. Treat, M.A. Brady, G. Smith, M.F. Toney, E.J. Kramer, C.J. Hawker, M.L. Chabinyc, Adv. Energy Mater. 1 (2011) 82-89.

[24] D. Chen, A. Nakahara, D. Wei, D. Nordlund, T.P. Russell, Nano Lett. 11 (2011) 561-571.

[25] J.S. Moon, C.J. Takacs, Y. Sun, A.J. Heeger, Nano Lett. 11 (2011) 1036-1039.

[26] K.H. Lee, P.E. Schwenn, A.R.G. Smith, H. Cavaye, P. E. Shaw, M. James, K.B. Krueger, I.R. Gentle, P. Meredith, P.L. Burn, Adv. Mater. 23 (2011) 766-770.

[27] C. Chen, F. Liu, C. Wang, A. Nakahara, T.P. Russell, Nano Lett., 11 (2011) 2071-2078.

[28] M. Brinkmann, Journal of Polymer Science Part B: Polymer Physics 49 (2011) 1218-1233.

[29] J. Clark, J.F. Chang, F.C. Spano, R.C. Friend, and C. Silva, App. Phys. Lett. 94 (2009) 163306.

[30] N.C. Greemham, X. Peng and A.P. Alivistaos, Phys. Rev. B 54 (1996) 17628-37.

[31] X.N. Yang, A. Alexeev, M.A.J. Michels and J. Loos, Macromolecules 38 (2005) 4289-95.

[32] A. Swinnen, I. Haeldermans, M. vande Ven, J. D`Haen, G. Vanhoyland, S. Aresu, M. D`Olieslaeger and J. Manca, Adv. Funct. Mat. 16 (2006) 760-5.

[33] F. Yang and S.R. Forrest, ACS Nano 2 (2008) 1022-32.

[34] N. Li, B.E. Lassiter, R.R. Lunt, G. Wei and S.R. Forrest, App. Phys. Lett. 94 (2009) 023307-3.

[35] (a) B.Q. Sun, H.J. Snaith, A.S. Dhoot, S. Westenhoff and N.C. Greenham, J. Appl. Phys. 97 (2005) 014914; (b) M. Campoy-Quiles, T. Ferenczi, T. Agostinelli, P.G. Etchegoin, Y. Kim, T.D. Anthopoulos, P.N. Stavrinou, D.D.C. Bradley and J. Nelson, Nat. Mater. 7 (2008) 158-64.

[36] C.M. Ramsdale, J.A. Barker, A.C. Arias, J.D. MacKenzie, R.H. Friend and N.C. Greehnam, J. Appl. Phys. 92 (2002) 4266-70.

[37] O.G. Reid, J.A.N. Malik, G. Latini, S. Dayal, N. Kopidakis, C. Silva, N. Stingelin and G. Rumbles, Journal of Polymer Science Part B: Polymer Physics (2011) DOI: 10.1002/polb.2237.

[38] (a) F.C. Spano, J. Chem. Phys. 122 (2005) 234701; (b) F.C. Spano, J. Chem. Phys. 126 (2007) 159901-1.

[39] F.C. Spano, Chem. Phys. 325 (2006) 22.

[40] J. Clark, C. Silva, R.C. Friend and. F.C. Spano, Phys. Rev. Lett. 98 (2007) 206404-6.